Applied Physics Research; Vol. 5, No. 2; 2013
ISSN 1916-9639 E-ISSN 1916-9647
Published by Canadian Center of Science and Education

# Monte Carlo Study of the Dynamic Screening Effect in Doped GaN

F. M. Abou El-Ela[1] & A. Z. Mohamed[1]

[1] Department of Physics, Faculty of Girls, Ain Shams University, Heliopolis, Cairo, Egypt

Correspondence: F. M. Abou El-Ela, Department of Physics, Faculty of Girls, Ain Shams University, Heliopolis, Cairo, Egypt. E-mail: fadlaeg@yahoo.com

Received: January 14, 2013 Accepted: February 16, 2013 Online Published: March 15, 2013

doi:10.5539/apr.v5n2p14 URL: http://dx.doi.org/10.5539/apr.v5n2p14

**Abstract**

Monte Carlo simulations of hot electron transport in n-type GaN when the interaction of the electrons with polar optical phonons is dynamically screened shows the effects of antiscreening at carrier densities of (1-5)x$10^{24}$ $m^{-3}$. At these densities full coupling between the Plasmon-phonon systems could be ignored to a first approximation together with degeneracy. Our calculations used the Lindhard formalism with Fermi-Dirac distribution and with neglecting the collisional damping when dynamic screened electron phonons scattering rates calculated. The screened scattering rate is strongly enhanced at low electron temperature and high carrier concentrations due to antiscreening property of inverse dielectric function. Antiscreening delays runaway and intervalley transfer to higher valleys. The peak drift velocity is enhanced and as result, so is the peak valley ratio.

**Keywords:** transport at high electric fields in semiconductors, screened optical phonon scattering rate, dielectric function and GaN transport

**PAcs No. 72.20Dp, 72.20 Ht, 77.22d**

## 1. Introduction

In the early 1970s, interest in GaN-based devices has risen rapidly. There has been considerable interest in GaN due to its wide band gap and favorable material properties, such as high electron mobility, very high thermal conductivity and a high breakdown (O'Leary et al., 2006). The large band gap energy of the III-nitrides insures that the breakdown electric field strength of these materials is much larger than that of other GaAs and Si. GaN and related compounds with aluminum and indium currently have great potential for applications in optoelectronics devices in the frequency range from microwaves to ultraviolet, quantum dots infrared photodetectors ( Chen & Wang, 2008; Dyson & Ridley, 2008; Lee et al., 2008; Limb et al., 2006; Averine et al. 2008; Butun et al. 2006 ). GaN also has large speed electron velocity and can be used for electronics devices of high power and high temperature field effect transistors (Look et al., 2001; Monyor et al., 2003).

The electron transport characteristics of the III–V nitride semiconductor, GaN, have long been recognized. Littlejohn et al. (1975) were the first to report results obtained from Monte Carlo simulations of the steady-state electron transport within bulk wurtzite GaN. Gelmont et al. (1993) reported on ensemble two-valley Monte Carlo simulations of the electron transport within bulk wurtzite GaN. Mansour et al. (1995) reported the use of such an approach in order to determine how the crystal temperature influences the velocity-field characteristic associated with bulk wurtzite GaN. Kolník et al. (1995) reported on employing full-band Monte Carlo simulations of the electron transport within bulk wurtzite GaN and bulk zincblende GaN. A more general analysis, in which transient electron transport within GaN, AlN, and InN was studied, was performed by Foutz et al. (1999).

Since many of today's interesting microelectronic devices are working in high doping concentrations up to $10^{25}$ $m^{-3}$, inclusion of dynamic screening has become very important. It has long been known that screening of the polar interaction between electrons and optical phonons occurs dynamically rather than statistically (Meyer & Bartoli, 1983; Ridley, 1985; Abou El-Ela et al., 1986; Abou El-Ela & Ridley, 1988; Lugli & Ferry, 1983; Lugli, 1985). Nevertheless, in most descriptions of the scattering by polar optical modes screening has been either regarded as negligible or treated statistically (Ehrenreich, 1959; Doniach, 1959; Ravich, 1971).

For carrier densities of $2\times10^{24}$ $m^{-3}$ and above in GaN screening becomes of considerable importance and its dynamics nature must be taken into account. A Full treatment would involve the effects due to coupling Plasmon-phonon system becomes strong at electron densities above $5\times10^{24}$ $m^{-3}$ , and there exists a regime of densities around $2\times10^{24}$ $m^{-3}$ in which screening effects are not negligible but the effect of coupling can be ignored. This regime turns out to be where the phenomenon of antiscreening is strong, and it may therefore be denoted the antiscreeening regime.

We explore the effect of antiscreening to model hot electron transport at high electric fields with aim of illuminating features such as the peak drift velocity, the peak to valley ratio, runaway, and the electron transfer negative differential resistance.

**2. Dynamic Screened Optical Phonon Scattering Rates**

At high doped GaN, the dynamic screening is highly favorable for polar optical phonon interaction due to it is dynamic nature. in GaN ,The polar optical phonon frequency $\omega_0$ is high and is different from that of the electron plasmon frequency $\omega_p$. Phase lags accurse if $\omega_p < \omega_0$ which produces what so called an anti screening effect. The interaction between an electron and the polar optical phonon is enhanced due to electron piling up on the potential peaks instead of the trough.

The effect of screening was described by the interaction screened potential. The potential is given by Ridley (1988)

$$\frac{v_s(\mathbf{q},\omega)}{v(\mathbf{q},\omega)} = \frac{k_\infty(\mathbf{q},\omega)}{k(\mathbf{q},\omega)}$$

where $v(q, \omega)$ and $v_s(q, \omega)$ are the interaction potential unscreened and screened (by free carriers) respectively, $k_\infty(q, \omega)$ is the high-frequency dielectric contribution from the valence band electrons and $k(q, \omega)$ is wave vector and frequency dependent dielectric function.

The rates for electron-screened phonon scattering are calculated (Ridley, 1988) using the limit of integral in both absorption and emission were given by Equations (2-4).

$$W(k) = \frac{e^2}{4}\frac{\omega_0\, m^{*1/2}}{2^{1/2}\pi\hbar\varepsilon_0}\left(\frac{1}{\varepsilon_\infty}-\frac{1}{\varepsilon_s}\right)\frac{1}{E_k^{1/2}}\left[n(\omega_0)\int_{x_{\min}}^{x_{\max}}\frac{[G(x,\omega)]^2}{x}dx + (n(\omega_0)+1)\int_{x_{\min}}^{x_{\max}}\frac{[G(x,\omega)]^2}{x}dx\right] \quad (1)$$

Where the first term represents the screened polar optical phonon absorption while the second term corresponds to screened polar optical phonon emission. In Equation (1), $\hbar\omega_0$ is the energy of the polar optical phonon, $\varepsilon_\infty$ is the high frequency optical dielectric constant, $\varepsilon_s$ is the relative static dielectric constant, $\varepsilon_0$ is the permittivity of free space and $m^*$ is the effective electron mass. The number of optical phonon will be given by Bose Einstein statistics. For simplicity, we assume that $\omega$ equals the longitudinal phonon frequency $\omega_0$. With following

$$x = \frac{q}{k_o} \qquad k_o = \left(\frac{2m^*\omega}{\hbar}\right)^{1/2}$$

$$G(\mathbf{q},\omega) = k_\infty(\mathbf{q},\omega)/k(\mathbf{q},\omega)$$

where the limits of integration for both absorption and emission of the screened polar optical phonon are

$$x_{\max} = \frac{q_{\max}}{k_0} = \left(\frac{E_k}{\hbar\omega_0}\right)^{1/2}\left[\left(1\pm\frac{\hbar\omega_0}{E_k}\right)^{1/2}+1\right] \quad (2)$$

$$x_{\min} = \frac{q_{\min}}{k_0} = \left(\frac{E_k}{\hbar\omega_0}\right)^{1/2}\left[\left(1+\frac{\hbar\omega_0}{E_k}\right)^{1/2}-1\right] \qquad \textit{absorption} \quad (3)$$

$$= \left(\frac{E_k}{\hbar\omega_0}\right)^{1/2}\left[1-\left(1-\frac{\hbar\omega_0}{E_k}\right)^{1/2}\right] \qquad \textit{emission} \quad (4)$$

$K(q, \omega)$ (dielectric function ) written as

$$k(\mathbf{q},\omega) = k_R(\mathbf{q},\omega) + i k_I(\mathbf{q},\omega) \quad (5)$$

The real part and imaginary part of dielectric function for Fermi-Dirac distribution are obtained after using dimensionless parameter, as

$$\frac{k_R(\mathbf{q},\omega)}{k_\infty(\mathbf{q},\omega)} = 1+\frac{3}{8}\,\frac{\gamma^2}{\Delta_o^{3/2}}\,\frac{1}{x^3}\int_0^\infty y\,\frac{1}{1+\exp\left[\theta(y^2-\Delta_f)\right]}\,\ln\left[\frac{(1+\frac{x}{2y})^2-\frac{1}{4x^2y^2}}{(1-\frac{x}{2y})^2-\frac{1}{4x^2y^2}}\right]dy \tag{6}$$

$$\frac{k_I(\mathbf{q},\omega)}{k_\infty(\mathbf{q},\omega)} = \frac{e^2 m^{*2}\, k_B T_e}{2\pi\ \varepsilon_\infty \hbar^4 q^3}\ \ln\left[\frac{1+\exp\left(\frac{-m^*}{2\hbar^2\mathbf{q}^2 k_B T_e}\left(\frac{\hbar^2\mathbf{q}^2}{2m^*}-\hbar\omega\right)^2+\frac{E_f}{k_B T_e}\right)}{1+\exp\left(\frac{-m^*}{2\hbar^2\mathbf{q}^2 k_B T_e}\left(\frac{\hbar^2\mathbf{q}^2}{2m^*}+\hbar\omega\right)^2+\frac{E_f}{k_B T_e}\right)}\right] \tag{7}$$

We use the dimensionless variables

$$\gamma = \frac{\omega_p}{\omega} \qquad \omega_p = \left(\frac{Ne^2}{\varepsilon_\infty m^*}\right)^{1/2} \qquad \theta = \frac{\hbar\omega}{k_B T_e}$$

$$y = \frac{k}{k_o} \qquad x = \frac{q}{k_o} \qquad k_o = \left(\frac{2m^*\omega}{\hbar}\right)^{1/2} \tag{8}$$

$$\Delta_f = \frac{E_f}{\hbar\omega} \qquad \Delta_o = \frac{E_{fo}}{\hbar\omega} \qquad E_{fo} = \frac{\hbar^2}{2m^*}\left(3\pi^2 N\right)^{2/3}$$

The Fermi-Dirac distribution becomes

$$f_o(E_\mathbf{k}) = [1+\exp[\theta\ (y^2-\Delta_f)]\ ]^{-1}$$

The inverse of dielectric function depends on both the wave vector q and the frequency of the phonon ω. $E_{f0}$ and $E_f$ define as Fermi energy at T = 0 and $T_e$ respectively at carrier concentration N where $T_e$ is the electron temperature.

A comparison between total polar optical phonon scattering rate and total screened polar optical phonon scattering rate for electrons in the central valley for various carrier concentrations for both electron and lattice temperature 300 K is presented in Figure 1. The screened scattering rate is enhanced with increasing carrier concentrations. This emphasizes the influence of antiscreening regime.

**3. Results and Discussion**

In our study we simulate 10000 electrons by using Monte Carlo method. The main types of scattering mechanisms included in our calculations are polar optical phonon scattering, acoustic phonon scattering, piezoelectric phonon scattering, equivalent intervalley phonon scattering and non- equivalent intervalley phonon scattering (Lugli, 1985; Jacoboni & Lugli, 1989; Abou El-Ela, 2002). Also, the screened polar optical phonon scattering is assumed to operate only in the central valley due to large electron effective mass in the other valleys.

The carrier concentrations chosen are around $4\text{x}10^{24}$ $m^{-3}$, and we believe it is safe enough to ignore the electron-plasmon couple mode interaction, up to used electron concentration. In addition, the pauli exclusion principle renders the phonon scattering rate and can neglected to simplify the calculations (Long, 1986). The Lindhard formalism (Ridley, 1988; Lindhard, 1954; Ziman, 1972) is a very good approximation to the dielectric function in the weak coupling limit; in additions to neglecting the collisional damping. Also, for simplicity nonparabolicity and the coupling between various electrons and holes have been neglected. The material parameters used for our simulations are tabulated in Table 1 while the valley parameters selections are presented in Table 2 (O'Leary et al., 2006; Lambrech, 1994).

The variation of steady state velocity with electric field for GaN is presented in Figure 2 for lattice temperatures 300 K, where a comparison between the polar phonon scattering (Pol) and the screened polar phonon scattering (Sc) at a carrier concentration $(1\text{-}5)\times10^{24}$ $m^{-3}$ has been shown. Application of a strong electric field accelerates the electron up to phonon energy, so that electron having reached this energy will immediately emit a phonon, thereby losing nearly all of its kinetic energy. The scattered electron with energy E = 0 was accelerated once again to E = ħω, and the same process is repeated thereafter until it is interrupted by other scattering agent. Such phenomenon is often referred to as a streaming motion. The drift velocity decreases relative to the unscreened case as a consequence of increase the carrier concentration in the first region of Figure 2 for electric fields between $(50\text{-}200)\times10^5$ V/m ; therefore, the streaming motion becomes highly favorable in this region. In the second region, at electric field above $200\times10^5$ V/m, the intervalley scattering becomes more effective in controlling the motion of the electron, while the electron temperature increases as a result of the energy gained from the field. In second region the drift velocity in screened cases increases compared to unscreened case due to Antiscreening delays runaway and intervalley transfer to higher valleys.

Other transport data collected during the M.C program for equilibrium state includes the electron average velocity in the central valley for lattice temperatures 300 K at carrier concentrations $(1\text{-}5)\times10^{24}$ $m^{-3}$ , shown in Figure 3.

The mean electron energy in central valley for lattice temperatures 300 K is presented in Figure 4 at a carrier concentrations $(1\text{-}5)\times10^{24}$ $m^{-3}$ for lattice temperatures 300 K. The mean electron energy for the screened case decreases with increasing carrier concentration due to the enhanced phonon emission.; meanwhile Figure 4 shows the influence of streaming motion in reducing the electron energy. The fractional electron number in the central valley for lattice temperatures 300 K at carrier concentrations $(1\text{-}5)\times10^{24}$ $m^{-3}$ is shown in Figure 5. As a result of quenching the electron energy in the central valley, the fractional electron number increases with increasing the carriers concentrations in screened polar optical.

In Figures (6-a, b, c) we presented the influence of screened polar optical phonon scattering at a carrier concentrations $(1\text{-}5)\times10^{24}$ $m^{-3}$ on the energy distribution for electric field $(70, 100, 250)\times10^5$ V/m. The electron energy is shifted to small energy for increasing electron densities, as result of the antiscreened polar optical phonon emission. A kink appears in the energy distribution at electron energy equal to the phonon energy. There is another kink at electron energy correspond to 2ħω, representing iterative emission of two phonons, which is possible only at lattice temperature 300 K. It is very important to notice the reduction of the number of electrons transferred to higher valley. This is in fact due to drop of electron average energy which becomes quite large at high carrier densities.

In Figure 7, the variation of the drift velocity with the electric field is presented at carrier and impurity concentrations of $5\times10^{24}$ $m^{-3}$ for lattice temperatures 300K ; in this figure we studied the influence of:

a- Polar optical phonon scattering.

b- Polar optical phonon scattering with impurity scattering (Imp scattering), (Ridley, 1988; Van de Roer, 1986) and electron- electron scattering (E-E scattering), (Bruentti, 1985).

c- Screened polar optical phonon scattering with both with impurity scattering (Imp scattering) and electron-electron scattering (E-E scattering).

Also acoustic phonon scattering and intervalley scattering are included; the results presented for lattice temperature of 300 K. The increase of the drift velocity in case of screened polar phonon scattering is not altered much with inclusion of E-E scattering and the impurity scattering.

Figure (8) showed the variation of the electron energy in the $\Gamma_1$ valley at carrier and impurity concentrations of $5\times10^{24}$ $m^{-3}$ for lattice temperatures 300 K. The electron average energy in the central valley decreases with the inclusion of both electron- electron scattering (E-E) and the impurity scattering. Therefore, the probability of the electron transfer to upper valley decreases resulting in an increase of the fractional number of the electron in central valley.

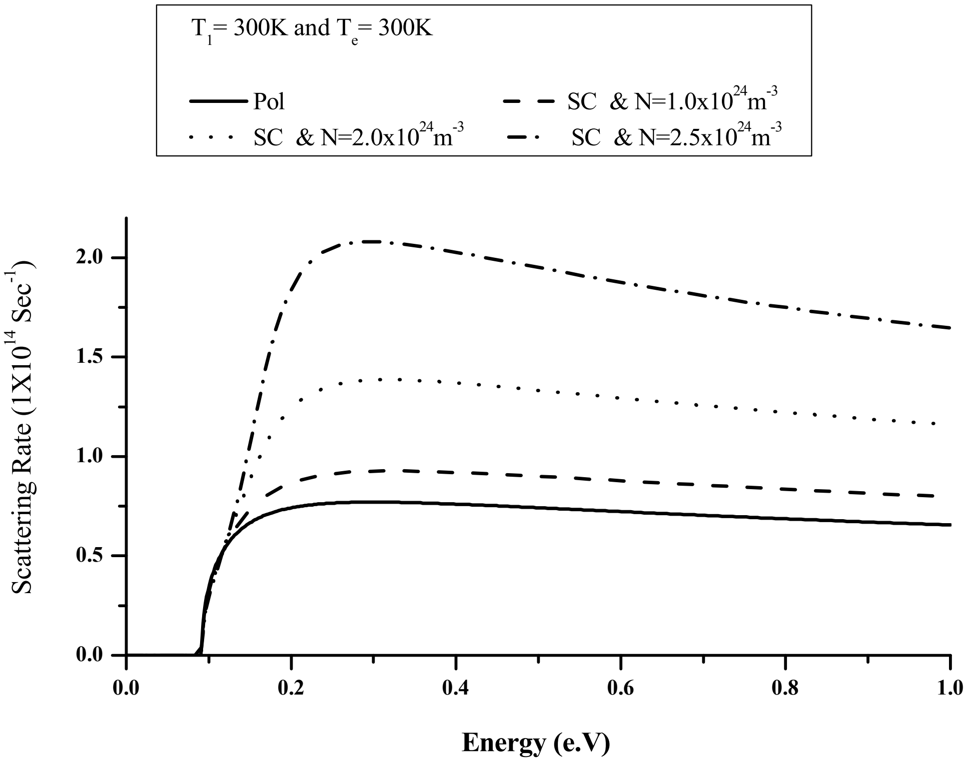


Figure 1. Scattring rate for polar phonon emission in the $\Gamma_1$ Valley against electon energy for various carrier concentrations

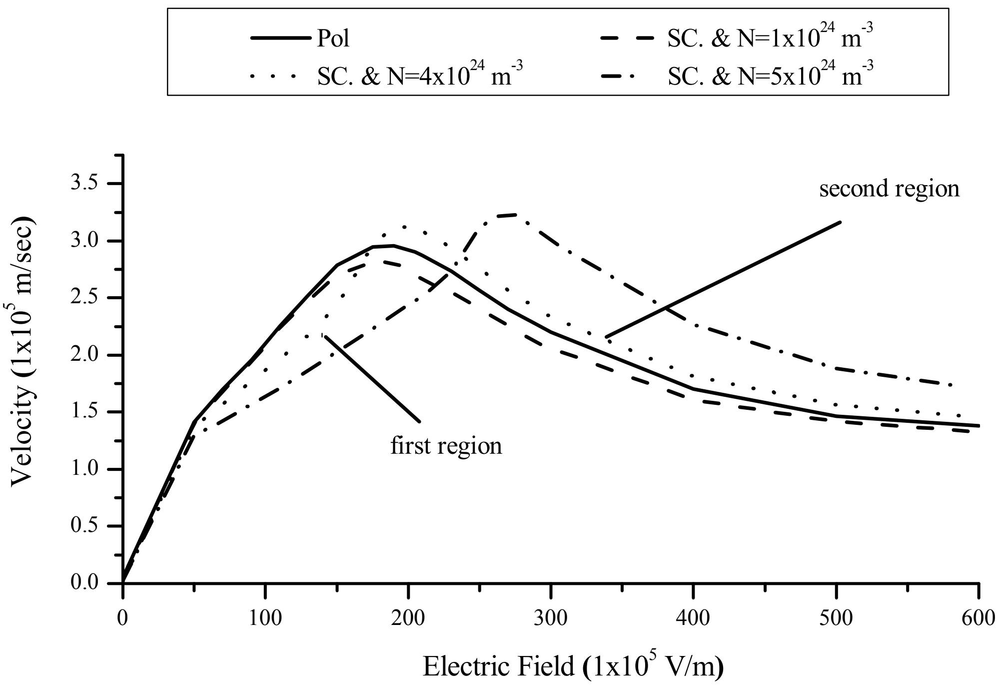


Figure 2. The total electron drift velocity versus electric field at 300 K

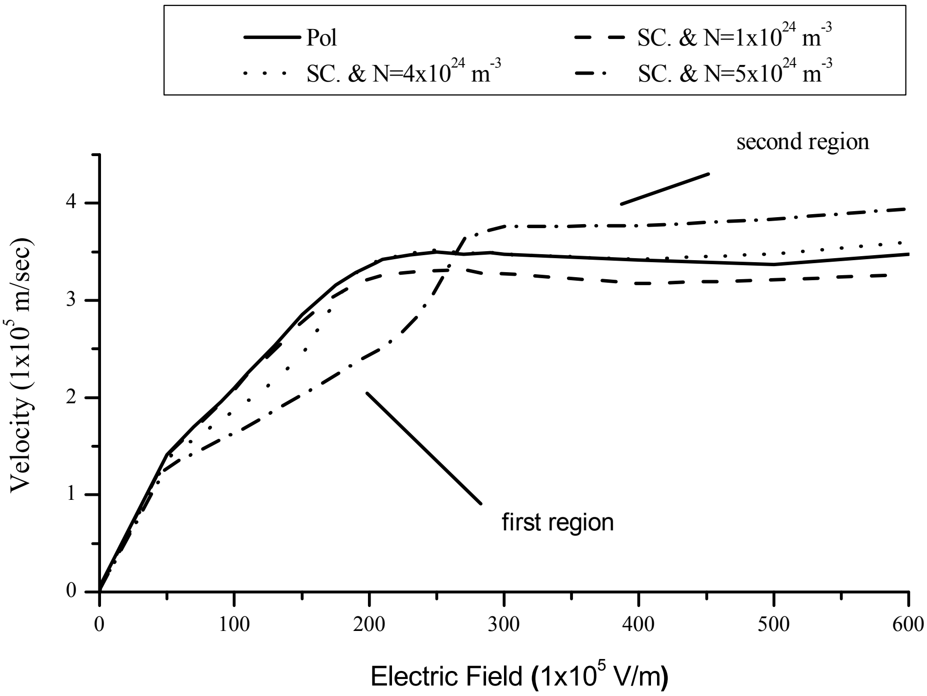


Figure 3. The average electron drift velocity versus electric field in the $\Gamma_1$ valley at 300 K

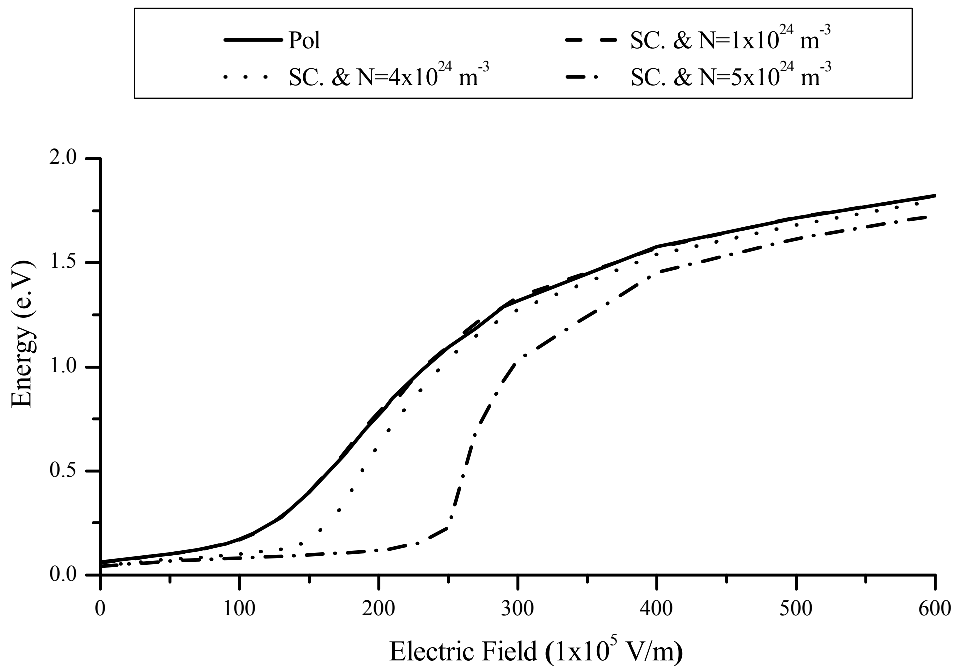


Figure 4. The average electron energy versus electric field in the $\Gamma_1$ valley at 300 K

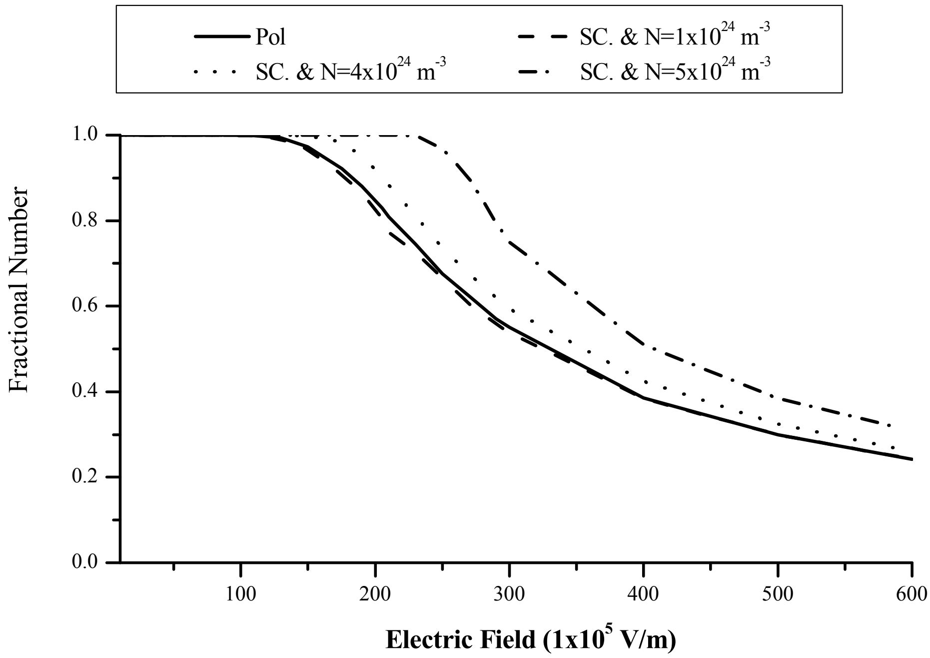


Figure 5. The freaction number of electron versus electric field in the $\Gamma_1$ valley at 300 K

Table 1. The material parameters corresponding to wurtzite GaN

| Parameter | Value |
|---|---|
| Mass density (kg/m$^3$) | 6150 |
| Sound velocity (m/s) | 6560 |
| Acoustic deformation potential (eV) | 8.3 |
| Static dielectric constant | 8.9 |
| High-frequency dielectric constant | 5.35 |
| Piezoelectric constant, $e_{14}$ (C/m$^2$) | 0.375 |
| Optical phonon energy (eV) | 0.0912 |
| Intervalley deformation potentials (eV/m) | $10^{11}$ |
| Intervalley phonon energies (eV) | 0.0912 |

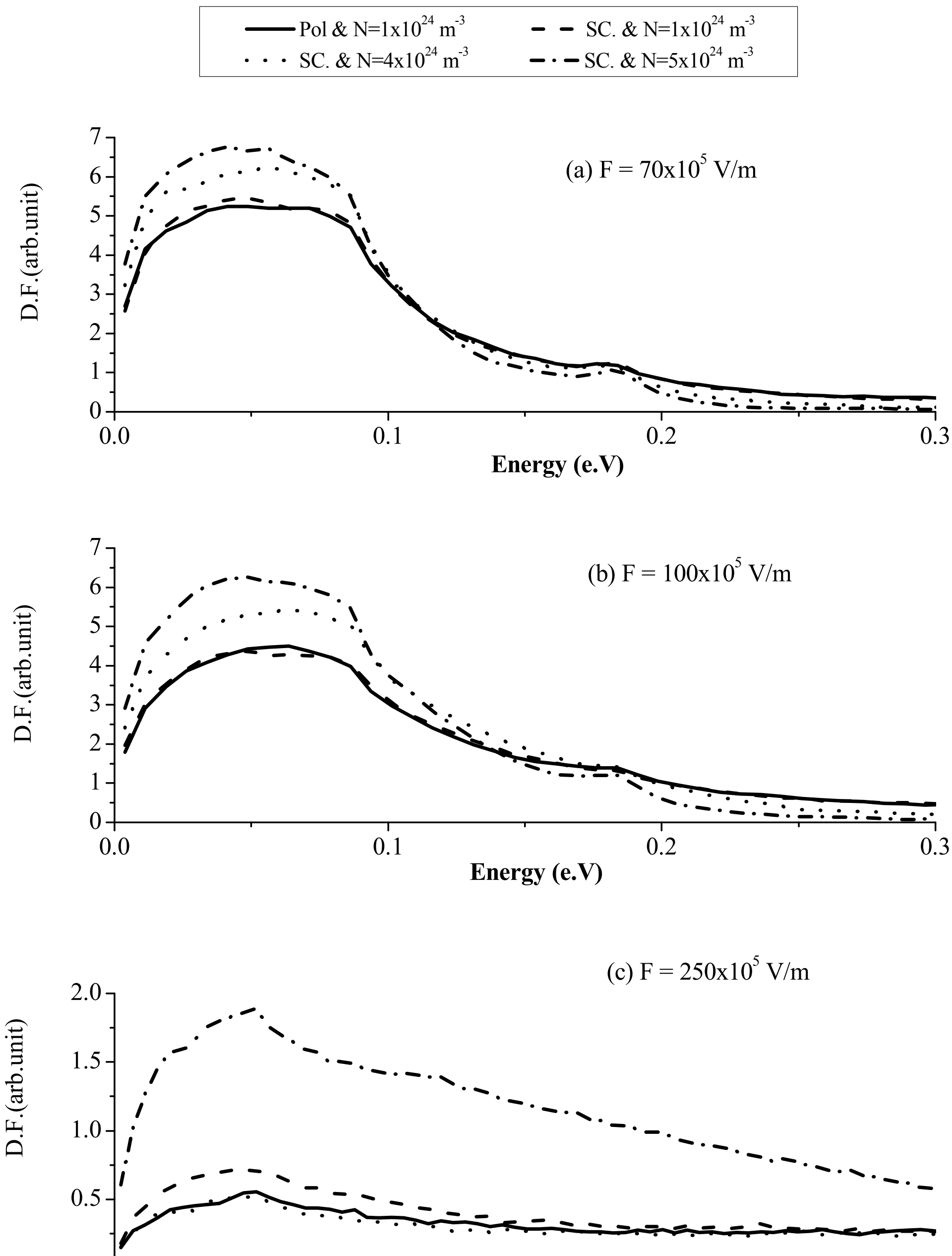


Figure 6. The number of D. F. versus electron energy in $\Gamma_1$ valley at 300 K

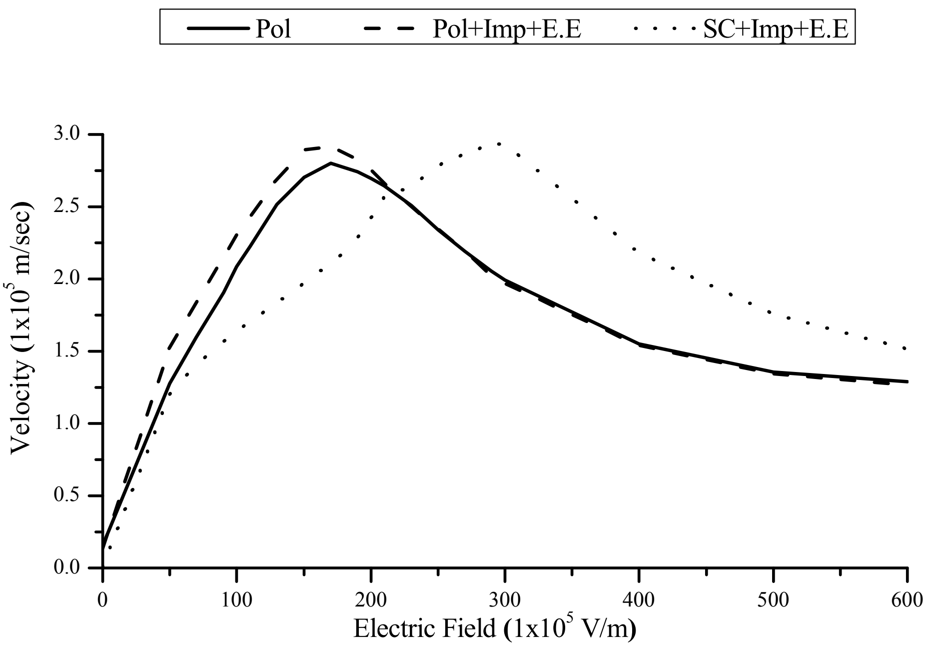


Figure 7. The total electron drift velocity versus electric field at 300 K in case of unscreened and screened polar optical phonons scattering

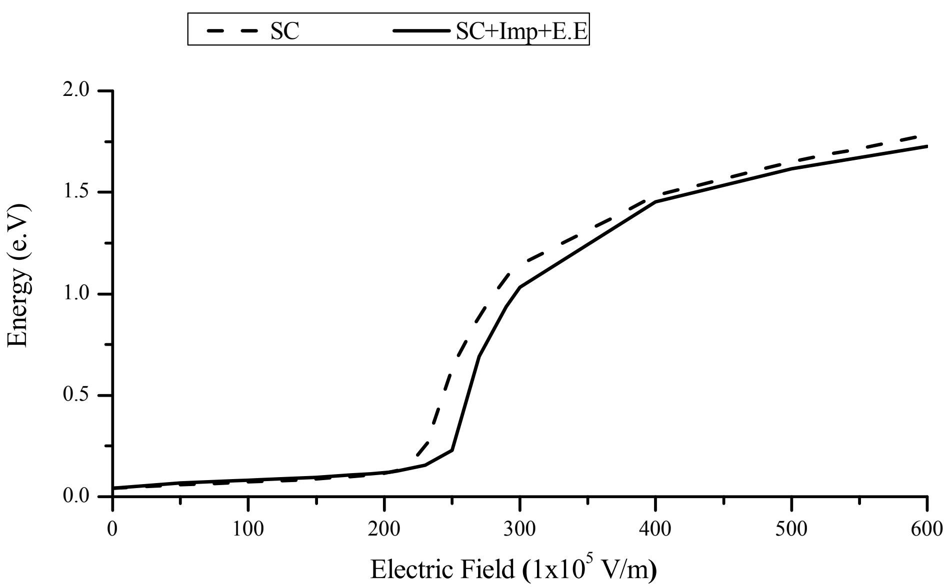


Figure 8. The average electron energy versus electric field in the $\Gamma_1$ valley at 300 K in case of screened polar optical phonons scattering

Table 2. The valley parameters corresponding to wurtzite GaN

| **Valley** | $\Gamma_1$ | $\Gamma_2$ | L-M |
|---|---|---|---|
| Valley degeneracy | 1 | 1 | 6 |
| Effective mass | 0.2 $m_e$ | $m_e$ | $m_e$ |
| Intervalley energy separation (eV) | --- | 1.9 | 2.1 |
| Energy gap (eV) | 3.39 | 5.29 | 5.49 |
| Nonparabolicity ($eV^{-1}$) | 0.189 | 0.0 | 0.0 |

## 4. Conclusions

The importance of including the dynamic screening in optical polar materials such as GaN increases especially at high carrier densities. We have calculated the screened scattering rate for GaN; the results showed enhancement of the scattering rate at high carrier densities, as a consequence of the strong antiscreening of polar phonon by the free carriers. The drift velocity at a given field increases with carrier concentration while the average energy decreases. This is mainly due to an enhancement of forward scattering rate even though the energy-loss rate is increased accompanied by antiscreening. A full account of hot electron transport in the antiscreening regime was investigated which included the role of charged impurity (statistical screened model) and E-E scattering. E-E scattering and charged impurity scattering leads to a moderation of the influence of antiscreening of polar optical phonon on the electron transport. E-E scattering has little influence on transport properties except leaning the distribution function towards a Maxwellian distribution.

## References

Abou El-Ela, F. M. (2002). Transport properties of ZnS:Mn at very high electric fields. *Indian J. of Phys., 76A*(4), 361.

Abou El-Ela, F. M., & Ridley, B. K. (1988). Hot carriers in semiconductor. *USA, Solid State Electronics, 314*, 691. http://dx.doi.org/10.1016/0038-1101(88)90369-3

Abou El-Ela, F. M., Riddoch, F. A., Davis, M., & Ridley, B. K. (1986). *Proc. Int. Conf. Semiconductor physics, Stockholm*, p.1567.

Averine, S. V., Kuznetzov, P. I., Zhitov, V. A., & Alkeev, N. V. (2008). Effect of optical excitation level on the MSM-detector high-speed response. *Solid-State Electron, 52*, 618. http://dx.doi.org/10.1109/UWBUS.2008.4669385

Bruentti, R., Jacoboni, C., Matulionis, A., & Dienys, H. (1985). *Physica, 134B*, 369.

Butun, S., Gokkavas, M., Yu, H. B., & Ozbay, E. (2006). Dual-color ultraviolet metal-semiconductor-metal AlGaN photodetectors. *Appl. Phys. Lett., 89*, 073503. http://dx.doi.org/10.1063/1.2358206

Chen, S. Y., & Wang, G. (2008). High-field properties of carrier transport in bulk wurtzite GaN: A Monte Carlo perspective. *Journal of Applied Physics, 103*, 023703. http://dx.doi.org/10.1063/1.2828003

Doniach, S. (1959). Lattice Screening in Polar Semiconductors. *Proc. Phys. Soc., London, 73*, 849. http://dx.doi.org/10.1088/0370-1328/73/6/303

Dyson A., & Ridley, B. K. (2008). High-field transport and terahertz generation in GaN. *Journal of Applied Physics, 104*, 113709. http://dx.doi.org/10.1063/1.3032272

Ehrenreich, H. (1959). Screening effects in polar semiconductors. *J. Phys. Chem. Solids, 8*, 130. http://dx.doi.org/10.1016/0022-3697(59)90297-5

Foutz, B. E., O'Leary, S. K., Shur, M. S., & Eastman, L. F. (1999). Transient electron transport in wurtzite GaN, InN, and AlN. *J. Appl. Phys., 85*, 7727. http://dx.doi.org/10.1063/1.370577

Gelmont, B., Kim, K., & Shur, M. (1993). Monte Carlo simulation of electron transport in gallium nitride. *J. Appl. Phys., 74*, 1818. http://dx.doi.org/10.1063/1.354787

Jacoboni, C., & Lugli, P. (1989). *The Monte Carlo method for semiconductor device simulation*. Wien: Springer-Verlag.

Jacoboni, C., & Reggiani, L. (1983). The Monte Carlo method for the solution of charge transport in semiconductors with applications to covalent materials. *Rev. Mod. Phys., 55*, 645. http://dx.doi.org/10.1103/RevModPhys.55.645

Kolnik, J., Oğuzman, I. H., Brennan, K. F., Wang, R., Ruden, P. P., & Wang, Y. (1995). Electronic transport studies of bulk zincblende and wurtzite phases of GaN based on an ensemble Monte Carlo calculation including a full zone band structure. *J. Appl. Phys., 78*, 1033. http://dx.doi.org/10.1063/1.360405

Lambrecht, W. R. L., & Segall, B. (1994). Electronic Structure of Diamond, Silicon Carbide, and the Group-III Nitrides. Properties of Group III Nitrides. In J. H. Edgar (Ed.), *EMIS Data reviews Series*, Chap. 4. http://dx.doi.org/10.1557/PROC-339-565

Lee, K. H., Chang, P. C., Chang, S. J., Yu, C. L., Wang, Y. C., & Wu, J. S. L. (2008). GaN MSM Photodetectors with an Unactivated Mg-Doped GaN Cap Layer and Sputtered ITO Electrodes. *Electrochem. Soc., 155*, J165. http://dx.doi.org/10.1149/1.2900102

Limb, J. B., Yoo, D., Ryou, J. H., Lee, W., Shen, S. C., & Dupuis, R. D. (2006). GaN ultraviolet avalanche photodiodes with optical gain greater than 1000 grown on GaN substrates by metal-organic chemical vapor deposition. *Appl. Phys. Lett., 89*, 011112. http://dx.doi.org/10.1063/1.2219390

Lindhard, J. (1954). *Dan. Vidensk. Selsk. Mat.- Fys. Medd., 28*, 8.

Littlejohn, M. A., Hauser, J. R., & Glisson, T. H. (1975). Monte Carlo calculation of the velocity-field relationship for gallium nitride. *Appl. Phys. Lett., 26*, 625. http://dx.doi.org/10.1063/1.88002

Long, A. P., Beton, P. H., & Kelly, M. J. (1986). Hot-electron transport in heavily doped GaAs. *Semicond. Sci. Technol., 1*, 63. http://dx.doi.org/10.1088/0268-1242/1/1/009

Look, D. C., & Sizelove, J. R. (2001). Predicted maximum mobility in bulk GaN. *Appl. Phys. Letters, 79*(8), 1133. http://dx.doi.org/10.1063/1.1394954

Lugli, P. (1985). *Electron-Electron Effect in semiconductor* (PhD, Thesis). Colarda State University, USA.

Lugli, P., & Ferry, D. K. (1983). Effect of electron-electron scattering on Monte Carlo studies of transport in submicron semiconductors devices. *Physica B, 117*, 251. http://dx.doi.org/10.1016/0378-4363(83)90497-7

Mansour, N. S., Kim, K.W., & Littlejohn, M. A. (1995). Theoretical study of electron transport in gallium nitride. *J. Appl. Phys., 77*, 2834. http://dx.doi.org/10.1063/1.358696

Meyer, J. R., & Bartoli, F. J. (1983). Dynamic dielectric response to electron-hole and electron-electron interactions. *Phys. Rev. B, 28*, 915. http://dx.doi.org/10.1103/PhysRevB.28.915

Monyor, E., Omnés, F., & Calle, F. (2003). *Semicond. Sci. Technol., 18*, R33-R51.

O'Leary, S. K., Foutz, B. E., Shur, M. S., & Eastman, L. F. (2006). Steady-State and Transient Electron Transport Within the III–V Nitride Semiconductors, GaN, AlN, and InN: A Review. *J. Mater. Sci.: Mater Electron, 17*(87). http://dx.doi.org/10.1007/s10854-006-5624-2

Ravich, Yu. I., Efimova, B. A., & Tamarchenko, V. I. (1971). Scattering of Current Carriers and Transport Phenomena in Lead Chalcogenides. *Phys. Status. Solidi B, 43*(11). http://dx.doi.org/10.1002/pssb.2220430102

Ridley, B. K. (1985). *Adv. Solid State Phys.* (Festkorperprobleme)*, 25*, 449, (1985).

Ridley, B. K. (1988). *Quantum Processes in Semiconductors*. Oxford: Claredon Press.

Van de Roer, T. G., & Widdershoven, F. P. (1986). Ionized impurity scattering in Monte Carlo calculations. *J. Appl. Phys., 59*, 813. http://dx.doi.org/10.1063/1.336603

Ziman, J. M. (1972). *The Principle of Theory of Solids.* Cambridge: Cambridge university press.